

A Competent Convolutional Sparse Representation Model for Pan-Sharpener of Multi-Spectral Images

Rajesh Gogineni¹, Girish Kumar Darisi²

¹ *Dhanekula Institute of Engineering & Technology, Ganguru, Andhra Pradesh- 521139*

² *Shri Vishnu Engineering College for Women, Bhimavaram, Andhra Pradesh-534202*

Abstract

Two types of images are produced by Earth observation satellites, each having complementing spatial and spectral characteristics. Pan-sharpening (PS) is based on remote sensing and image fusion approach that produces a high spatial resolution multi-spectral image by merging spectral information from a low spatial resolution multispectral (MS) image with intrinsic spatial details from a high spatial resolution panchromatic (PAN) image. Traditional pan-sharpening methods continue to seek for a fused image that contains the necessary spatial and spectral information. This work proposes a pan-sharpening method based on a recent invention, convolutional sparse representation (CSR). Geometric structural characteristics are extracted from the PAN image using a CSR-based filtering procedure. The challenge of learning filters, convolutional basis pursuit denoising (CBPDN), is handled using a modified dictionary learning method based on the concept of Alternating Direction Method of Multipliers (ADMM). The retrieved details are put into MS bands using applicable weighting coefficients. Because the proposed fusion model avoids the standard patch-based method, spatial and structural features are preserved while spectral quality is maintained. The spectral distortion index SAM and the spatial measure ERGAS improve by 4.4 and 6.2 percent, respectively, when compared to SR-based techniques. The computational complexity is reduced by 200 seconds when compared to the most recent SR-based fusion technique. The proposed method's efficacy is demonstrated by reduced-scale and full-scale experimental findings utilising the QuickBird and GeoEye-1 datasets.

Keywords: Image fusion; Pan-sharpening; Convolutional sparse representation; Dictionary filters; Dictionary learning.

*Corresponding author Email: rgogineni9@gmail.com

1. Introduction

Two important criteria separate Earth observation satellite images: spatial resolution and spectral resolution. The ability to differentiate structural characteristics in a photograph is measured in spatial resolution, which is defined as the shortest distance between two disjoint independent objects. Spectral resolution [1] refers to the bandwidth and sample rate at which the sensor acquires information about the scene. Due to technological and physical limits, remote sensing devices provide images with a trade-off between spatial and spectral resolutions. The majority of high-resolution optical sensors, such as IKONOS, QuickBird, and Worldview, provide a Panchromatic (PAN) image with low spectral resolution but high spatial resolution, as well as a Multi-Spectral (MS) image with low spatial resolution but high spectral resolution. The MS and PAN photos were taken over the same area at the same time, so the two photographs depict the same scene.

Change detection, object recognition, land-cover and land-use classification are some of the remote sensing applications that necessitate high resolution MS (HRMS) images with high spatial and spectral resolution [2-3]. Image fusion is a crucial technique for merging complementary data from many input photos to create a composite image. Pan-sharpening (PS) is a widely used remote sensing image fusion technique that aims to create an HRMS image that is superior for human and machine perception than the individual input images. The purpose of PS is to create an HRMS image with the spatial quality of a PAN image but the spectral richness of an MS image.

For more than three decades, academics have been working on remote sensing image fusion to solve the problem of pan-sharpening. Traditional PS methods include component substitution (CS) and multi resolution analysis (MRA) based methodologies [4]. This study aims to demonstrate the CSR scheme and its benefits in pan-sharpening in a straightforward and simple manner. The following is the paper's outline. The basics of traditional PS approaches, as well as the notions of SR and CSR, are discussed in Section 2. Section 3 depicts the pan-sharpening approach based on CSR. Section 4 depicts the results and discussions from the smaller scale and full scale experiments. The paper comes to a close with Section 5.

2. Background

2.1. The generalized formulation for CS and MRA methods

The CS and MRA approaches can be abstractly explained while highlighting the implementation strategy. Let X_k be a number between 1 and 2, and k to be a number between 1 and 2.... N represents the MS image with N bands, while Y represents the PAN image. \bar{X}_k is the estimated HRMS picture, and \tilde{X}_k represents the MS image up-sampled to the size of the PAN image. Adding a detail image, D , to the up-sampled image, \tilde{X}_k , yields the pan-sharpened image.

$$\bar{X}_k = \tilde{X}_k + g_k \cdot D; k = 1; 2 \dots N \quad (1)$$

The detail picture, D , contains spatial information that isn't visible in the MS image bands. The image's dimension, D , is the same as the dimensions of the interpolated MS image and the fused image. The essential distinction between the CS and MRA techniques is the synthesis process by which the detail image, D , is estimated. The detail image determines the quality of the fused image. $g_k = [g_1, g_2 \dots g_N]$ is a vector of band-specific injection gains in Eq. (1). The detail image is expressed as, in CS-based approaches.

$$D = Y - \sum_{k=1}^N \omega_k \tilde{X}_k \quad (2)$$

The specific CS algorithm determines the selection of parameters such as injection gains (g_k) and the weight vector (k). For the weighted sum of MS bands, the weight vector k specifies the proportion of each band that must be preferred. Spectral distortion in the fused image is determined by the difference between the PAN image and the weighted sum of MS bands. Intensity-hue-saturation (IHS), principal component analysis (PCA), and the Gram-Schmidt transform (GS) are only a few of the most well-known CS-based approaches [5-6]. For MRA-based techniques, the following is a detail image:

$$D = Y - Y_L \quad (3)$$

Y_L stands for the low-pass version of PAN image Y . The type of filter used to determine Y_L and the injection gain vector g_k is determined by the MRA algorithm. Some of the most well-known MRA approaches are wavelets, 'atrous' wavelet transform (ATWT), additive wavelet luminance proportional (AWLP), curvelet transform, and contourlet transform [7].

The CS are noted for its ability in preserving the requisite geometric features, but the fused image suffers from spectrum distortion. MRA methods, on the other hand, are capable of increasing spectral information but fall short of CS methods in terms of spatial detail enhancement. Since the reconstruction of an image from its sparsifying representation possesses super-resolution capability and robustness, the sparse representation (SR) technique has recently been widely used to improve fusion quality.

3.2. Sparse representation

Natural signals like images are uncommon in the dictionary, a redundant image domain. The image can be represented by a linear combination of a few dictionary atoms (columns) [8-9]. Let $s \in \mathbb{R}^n$ be a small patch of an image of size $\sqrt{n} \times \sqrt{n}$, and $D \in \mathbb{R}^{m \times n}$ represent an over-complete dictionary, i.e., $n \ll m$: The image patch, s (which is defined as having a consistent structure), can be written as $s = D\alpha$, where α is a coefficient vector with the fewest non-zero members feasible. This method is performed for the complete image S , which consists of P number of image patches, in an iterative manner. The sparse representation theory provides a model for estimating the coefficient vector, as shown in [10]:

$$\hat{\alpha} = \operatorname{argmin} \|\alpha\|_0 \quad \text{s.t.} \quad \|S - D\alpha\|_2^2 = 0 \quad (4)$$

Where, $\|\cdot\|_0$ is the l_0 -norm that counts the number of non-zero entries. If α is adequately sparse, the optimization problem in Eq. (4) can be well approximated by replacing l_0 norm with the l_1 norm (of the vector α) as [11],

$$\hat{\alpha} = \operatorname{argmin} \|\alpha\|_1 \quad \text{s.t.} \quad \|S - D\alpha\|_2^2 \leq \epsilon \quad (5)$$

Here, ϵ is the error tolerance expressed as an upper bound for the sparse approximation error $\|S - D\alpha\|_2^2$. Several sparse representation methods [12] can efficiently handle the l_1 -norm problem as described in Eq. (5). The Orthogonal Matching Pursuit (OMP) iterative technique is employed in this paper [13]. The OMP technique is a greedy iterative method for estimating the sparse coefficient vector α for a given image patch. The basic idea behind this technique is to discover the non-zero points of the sparse coefficients vector α one by one in Eq (5).

The initial residual is assumed to be the training signal's'. The method searches the dictionary D for a specific column (atom) that best correlates with the current residual at each step. The residual is then iteratively updated by taking into account the new atom and its associated coefficient. The Least-Squares approach is used to update all non-zero coefficients throughout each iteration of the algorithm. An OMP algorithm's main advantages are its ease of implementation and speed of execution.

3.3. SR based PS methods

The first SR-based pan-sharpening solution was proposed by Li and Yang [14], and it was regarded as a restoration problem. The fused image patches are thought to be sparse when compared to a dictionary constructed from random patches derived from HRMS images in this technique. The required size and technique for dictionary generation results in a high computational cost in order to attain appropriate fusion quality. There's also the possibility that the HRMS image patches aren't present. The creation of a suitable lexicon is the most difficult challenge in SR-based PS approaches. Based on the type of image patches used for dictionary creation, there are two sorts of pan-sharpening methods: (i) The lexicon is constructed using patches from both the PAN and MS images [15-16]. (ii) The PAN image patch dictionary and its low-resolution counterpart [17-18]. Ayaset al. [19] proposed a single concise language for improving pan-sharpened image fusion quality. The sparse representation (SR)-based approaches [20, 21] are expected to outperform the traditional and model-based PS methods. The SR-based techniques, on the other hand, have the following flaws.

- i. Most SR-based pan-sharpening systems use a patch-partitioning approach, with individual patch processing ignoring the consistency restriction. When reconstructing images, the averaging process is used on overlapped patches, resulting in the loss of the image's spatial structure.
- ii. Sparse representation on overlapped patches produces a multi-valued representation (the representation generates different values for a given feature existing in the original image due to the processing of overlapped patches), which is not ideal for the full image.
- iii. SR-based approaches are susceptible to source image mis-registration. The sparse coefficients evaluated for particular patches may not be able to approximate the inherent characteristics of source images if the images are mis-registered. It results in pseudo-Gibbs phenomenon (Ex: ringing artefacts) in fused image at the mis-registered regions.
- iv) The primary challenge with PS approaches is that the basic implementation mechanism lacks the ability to define the link between source and fused images. A newly developed signal decomposition strategy called as convolutional sparse representation (CSR) is presented in detail to overcome these difficulties in existing pan-sharpening methods. Instead of considering specific patches repeatedly, CSR models the entire image, preserving spatial organisation and resulting in a single-valued representation.

3.4. Convolutional sparse representation

Zeiler et al. [22] established the convolutional form of representation as a tool for changing convolutional neural networks. Convolutional sparse representation (CSR) is an alternative representation of SR for accomplishing a convolutional decomposition of an entire picture when a sparsity constraint is applied. The primary purpose of CSR is to describe an image as a convolution of unknown coefficient maps $\{x_m\}$ and their corresponding dictionary filters $\{d_m\}$. CSR is used to model the entire picture S by regularising x_m with a sparsity prior.

$$\operatorname{argmin} \frac{1}{2} \|d_m * x_m - S\|_2^2 + \lambda \|x_m\|_1, m=1, 2, \dots, M \quad (6)$$

The symbol '*' symbolises convolution operation, whereas λ is a regularisation parameter (a scalar) that regulates the balance between sparsity and reconstruction error. The letter M stands for the number of dictionary fitters. A finite number of training photos is used to learn the dictionary filters.

$$\operatorname{argmin} \frac{1}{2} \|d_m * x_m - s_k\|_2^2 + \lambda \|x_m\|_1, \text{ s.t. } \|d_m\|_2 = 1 \quad (7)$$

The training images needed to learn dictionary filters are denoted by s_k . The coefficient maps, x_m , can well preserve the spatial structures in images, and the learnt dictionary filters give relatively moderate redundancy. The CSR model in Eq. (6) can be thought of as a convolutional form of Eq. (7), and is referred to as CBPDN (convolutional basis pursuit denoising). Many methods have been developed in the literature to address the CBPDN problem, with the alternate direction method of multipliers (ADMM) framework proving to be the most efficient [23, 24]. The CSR model was established to look at shift-invariant sparse representation, which is still a valuable feature in image fusion. Furthermore, the sparse representation for the entire image is calculated, resulting in a single-valued and optimal representation. CSR can avoid the duplication caused by overlapped pixels by learning the filters from the complete image, as shown in SR-based approaches. These features moderately maintain spatial structure consistency in the merged image.

4. Pan-sharpening based on CSR

There are three basic processes in the process of pan-sharpening multi-spectral photographs. (i) Increase the size of the MS image to that of the PAN image. (ii) From the PAN image, extract the high frequency detail (HFD) image. (iii) Injecting the HFD into the up-sampled MS image bands to reconstruct the HRMS image. The intensity changes that correspond to the geometric structures (edges, texture information) included in the PAN image are usually indicted by the high frequency detail image. As a result, the desired spatial features are the same as in the HFD image. By modifying the MATLAB function 'imresize' and using bicubic interpolation as a parameter, the MS picture bands are up-sampled to the size of the PAN image. The intensity component, I , is estimated from the MS image bands as,

$$I = \sum_{k=1}^N \tilde{X}_k \quad (8)$$

The histogram matching operation is performed between PAN image Y , and the obtained intensity component I , which results in new panchromatic image, \bar{Y} . The histogram matching process assists in reducing the inhomogeneity exists in spatial features present between the PAN image and MS image bands.

The dictionary filters D_h are learned from the high pass version (\bar{Y}_h) of the equalized PAN image \bar{Y} as

$$\underset{\{D_h\}}{\operatorname{argmin}} \quad 1/2 \|\sum_m D_h^m * \alpha_m - \bar{Y}_h\|_2^2 \quad \text{s.t.} \quad \|D_h^m\|_2 = 1 \quad (9)$$

The high pass version, $\bar{Y}_h = \bar{Y} - \bar{Y} * \text{flp}$, in which $*$ represents convolution operator, with flp is a low pass filter, namely Gaussian or Laplacian mask. The conventional approach to solve the above problem is based on alternating minimization with respect to parameters, such as coefficients vector α and the dictionary filters D_h . This problem can be efficiently solved by an Augmented Lagrangian framework with efficient solution of linear systems [25]. With the estimated dictionary filters D_h^m , the coefficients for the original PAN image, α_p are estimated as,

$$\underset{\{\alpha_p\}}{\operatorname{argmin}} \quad 1/2 \|\sum_m D_h^m * \alpha_p^m - \bar{Y}\|_2^2 + \lambda \sum_m \|\alpha_p^m\|_1 \quad (10)$$

The HFD image is evaluated as,

$$\text{HFD} = \sum_m D_h^m * \alpha_p^m \quad (11)$$

Finally, the HRMS image is reconstructed by injecting the HFD into each MS band that has been up-sampled, as seen below.

$$\hat{X}_k = \tilde{X}_k + \omega_k \cdot \text{HFD} \quad (12)$$

Where, $\omega_k = \frac{X_k}{\sum_{k=1}^N \tilde{X}_k}$, are the injection coefficients. The value of ω_k assists in injecting the band specific details. The contribution of each band to the multi-spectral image is used to formulate the spatial details injection technique. Fig.1 shows a schematic illustration of a pan-sharpening strategy based on CSR.

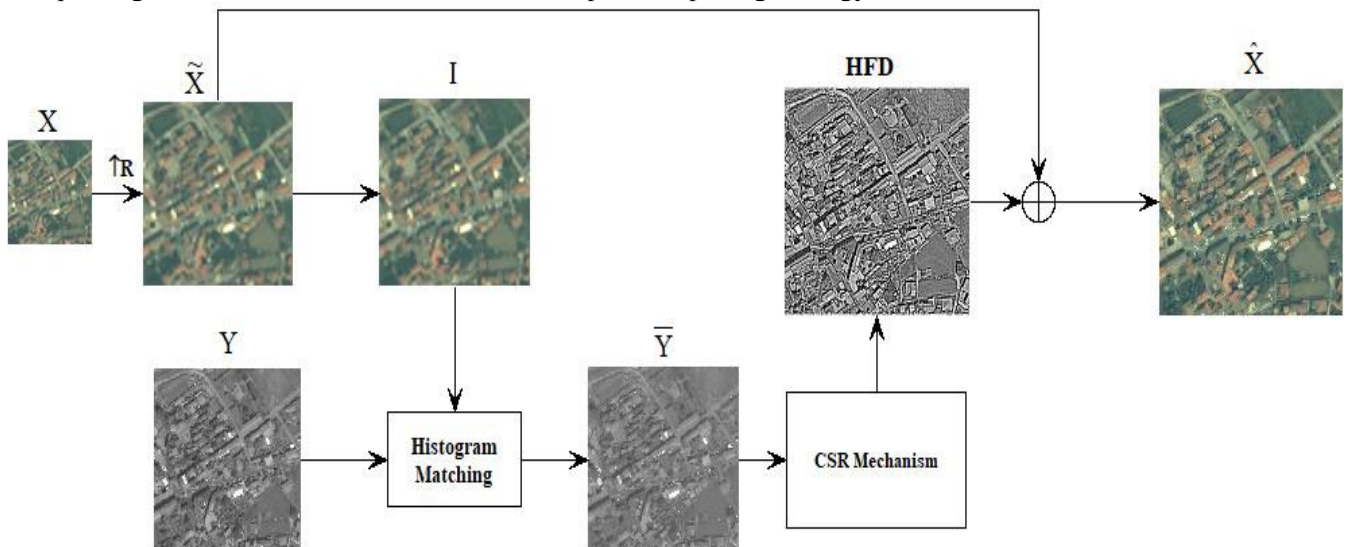


Figure 1: CSR based Pan-sharpening approach.

5. Results and Discussion:

5.1. Reduced-scale experimentation

While preserving the spectrum information of the MS image, the HRMS image should have the spatial features of a PAN image. To compensate for the lack of a reference image, various performance evaluation methodologies have been developed. This work [26] adapts the well-known Wald et al. technique for assessing the quality of the fused image at a lower size. In this technique, the source images (PAN and MS) are decimated by a factor equal to the resolution ratio of the PAN and MS images. The MS image is then resized to fit the PAN image's dimensions. The fusion process is done to damaged photographs, and the resulting image is compared to the original MS image, which serves as a reference image.

Four different notable SR methods are used for the assessment of the proposed method: SR-Li, SR-D Four different quality metrics are used for the performance evaluation of the CSR based pan-sharpening method [14, 15].

- I. The spectral angle mapper (SAM) calculates the amount of spectral distortion in terms of the absolute angle between the reference and fused image spectral vectors. If the two images are spectrally identical, the SAM value is zero.
- II. The universal image quality index (Q) determines how comparable two images are. Q4 is a multi-spectral extension of Q that may be used on photos with four bands. Each band's correlation, mean bias, and contrast variation make up Q4.
- III. The global error index ERGAS (relative dimensionless global error in synthesis) is a global error index. Lower ERGAS scores suggest multi-spectral band similarity.
- IV. Correlation coefficient (CC), indicates the overall quality.

For the reduced-scale study, two datasets from IKONOS and GeoEye-1 sensors were employed. Sub scenes are 1024×1024 pixels for PAN images and $256 \times 256 \times 4$ pixels for MS images. Because the resolution ratio for the considered datasets is four, these sub scenes are filtered and decimated by a factor of four. Pan-sharpening is applied to decimated data, such as an interpolated MS image ($256 \times 256 \times 4$) and its equivalent PAN image (256×256). The MS and pan-sharpened images are displayed using a red, green, and blue band composition. Each dictionary filter is 8×8 , and the total number of dictionary filters is 32 for reduced-scale experimentation and 64 for full-scale exploration.

Fig. 2 & 3 demonstrate the reduced-scale outcomes of the CSR-based pan-sharpening method for the GeoEye-1 and IKONOS datasets, respectively. The PAN image, the original MS image, and the MS image interpolated to the size of the PAN image are shown in Fig. 2(a), 2(b), and 2(c), respectively.



Figure 2: Visual outcomes of GeoEye-1 data at reduced scale (a) PAN image (b) Original MS image (c) Interpolated MS image (d) SR-Li (e) SR-D (f) PS-MSLD (g) SR-CD (h) Proposed CSR model.

Fig. 2(d) - 2(g) shows the pan-sharpened pictures derived from the most popular SR-based techniques (g). Spectral is readily obvious from the tree areas in the fused image created by the SR-Li method, as illustrated in Fig. 2(d). In the fused images acquired by the SR-D and PS-MSLD approaches, blocking effects may be noticed, particularly in the building region. The proposed strategy, like the SR-CD method, outperforms the others tested. In terms of spectral components, the proposed CSR technique (Fig.2 (h)) preserves the spatial information of the PAN image and appears to be pretty near to the interpolated MS image (colours). It represents the least amount of spectrum distortion, which is supported by the quantitative results in Table 1.

Table 1: Reduced-scale quantitative results for GeoEye-1.

	SR-Li	SR-D	PS-MSLD	SR-CD	Proposed CSR
Q4	0.8735	0.8911	0.9138	0.9242	0.9286
SAM	3.4213	3.3876	3.2735	3.2583	3.1127
ERGAS	3.1653	3.2715	3.1263	3.1098	2.9986
CC	0.8657	0.8892	0.9275	0.9289	0.9316

The visual consequences obtained using the QuickBird dataset at lower resolution are shown in Fig. 3. The variations in outcomes of contrasted procedures are difficult to discern from the visual findings. As a result, a piece of the image is zoomed and presented in the bottom left corner for each result. When the zoomed portion of multiple photos is examined, it becomes clear that the proposed CSR approach preserves spatial features better.

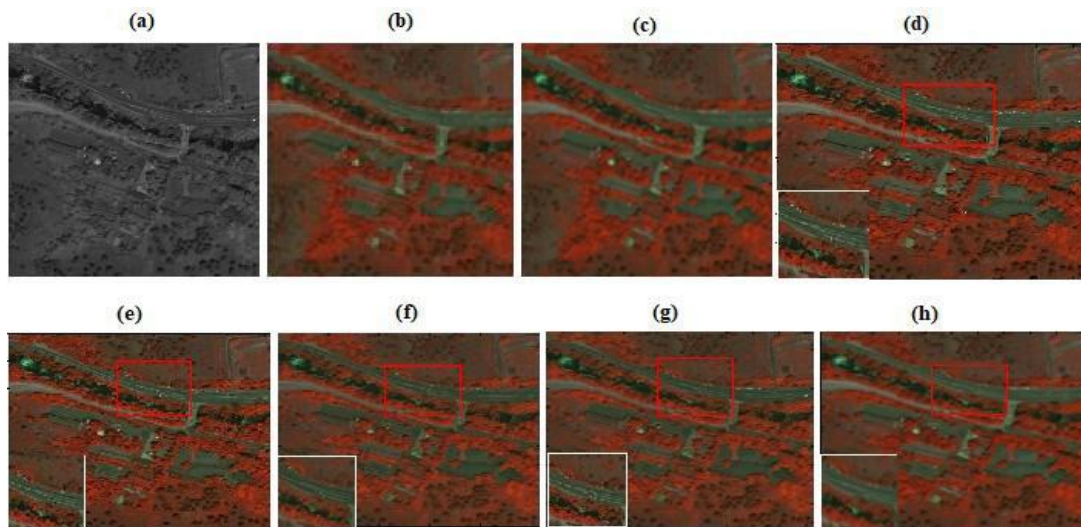


Figure 3: Visual outcomes of QuickBird data at reduced scale (a) PAN image (b) Original MS image (c) Interpolated MS image (d) SR-Li (e) SR-D (f) PS-MSLD (g) SR-CD (h) Proposed CSR model

The quantitative results in Table 2, particularly the metrics Q4 and CC values, show that the overall quality of the proposed method's pan-sharpened result has improved and the geometric details have been heightened. The retention of geometric features in the SR-Li, SR-D, and PS-MSLD results is low when compared to the suggested method, as evidenced by zoomed areas of the results. In the SR-CD method's result, the details surrounding the road are slightly blurred. The proposed method's superiority is supported by both visual and quantitative data. The reduced scale findings from two separate datasets, as well as the quantitative results, show that the suggested method's balance of spatial and spectral properties in the fused image is acceptable when compared to previous approaches.

Table 2: Quantitative results for QuickBird at reduced scale

	SR-Li	SR-D	PS-MSLD	SR-CD	Proposed CSR
Q4	0.8914	0.8986	0.9124	0.9241	0.9283
SAM	2.8764	2.8913	2.8565	2.8341	2.8175
ERGAS	3.2187	3.0187	3.1094	2.9973	2.9818
CC	0.9121	0.9236	0.9288	0.9345	0.9429

5.2. Full-scale experimentation

The full-scale assessment, which is composed of two metrics: spectral distortion index D and spatial distortion index D_s [27], is estimated using the quality with no reference (QNR) approach. The quality metric QNR, on the other hand, infers the similarity measure. The fusion technique is used on the original dataset without shrinking the source images; however, the MS image is up-sampled to match the size of the PAN image.

Another QuickBird dataset's full-scale results are shown in Fig.4. The PAN image of size 512 512 pixels is shown in Fig.4 (a). Fig. 4(c) shows an MS image that has been interpolated to the size of a PAN image. The original MS image, with a size of 128 x 128 pixels, is shown in Fig.4 (b).

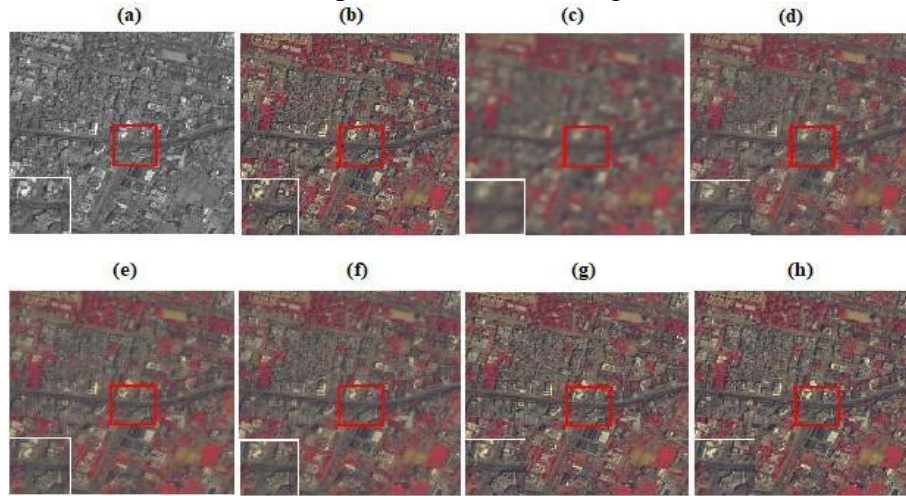


Figure 4: Visual outcomes of QuickBird data at full scale (a) PAN image (b) Original MS image (c) Interpolated MS image (d) SR-Li (e) SR-D (f) PS-MSLD (g) SR-CD (h) Proposed CSR model

In comparison to the original data, the proposed CSR technique did a better job of conserving spectral information and improving spatial details. Table 3 shows the quality metrics that coincide. The visual and quantitative results support the pan-sharpening method's ability to preserve spectral purity while sharpening spatial features. In the pan-sharpened image of the proposed CSR approach, the road part and the margins of the buildings encompassed in red coloured boxes are consistent. The SR-Li and PS-MSLD approaches, on the other hand, smooth out the details. The blurring effect is created via the SR-D approach, as evidenced by the concentration on magnified regions. The numerical findings show that the suggested method outperforms the SR-based strategies that were compared. The proposed method has the lowest values for the distortion indices and the highest value for the overall quality index QNR, indicating that it outperforms the other described methods.

Table 3: Quantitative results for QuickBird at full scale

	SR-Li	SR-D	PS-MSLD	SR-CD	Proposed CSR
D_λ	0.1186	0.1124	0.1093	0.1058	0.1021
D_S	0.0893	0.0792	0.0687	0.0611	0.0587
QNR	0.8027	0.8173	0.8295	0.8396	0.8452

5.3. CSR model performance analysis

The performance of pan-sharpening is evaluated in this work using various numbers of dictionary filters, D_m . For dictionary filters, we utilised the numbers 16, 32, 64, and 128. The best fusion quality for the datasets is achieved by using 32 filters at reduced scale and 64 filters at full scale. The filter has been set to a size of 8×8 pixels. The regularisation parameter is set to 0.01 for both smaller and full-scale experiments. The notion of filter size is chosen for this experiment based on the orthogonal matching pursuit sparse coding technique's criteria (OMP). Other implementation details are chosen as detailed in [24] in order to achieve the greatest performance.

The SR based methods adapt patch based processing strategy, hence pan-sharpening process consume more time. When compared to most SR-based PS systems, CSR-based pan-sharpening takes significantly less time to deploy. The Table depicts the execution time analysis for the reported methods.

Table 4: Execution timing analysis of the reported methods

	SR-Li	SR-D	PS-MSLD	SR-CD	Proposed CSR
Time (sec)	1875	1065	854	673	465

6. Conclusion

Pan-sharpening is a popular remote sensing image fusion technique for combining spatial and spectral characteristics that aren't visible in a single image. The pan-sharpening approach produces high resolution multi spectral (HRMS) pictures, which are frequently utilised in feature extraction, classification, and other applications. The traditional CS, MRA, and more contemporary SR-based approaches have made significant progress in achieving a fused image with acceptable features. However, a pan-sharpening paradigm that achieves a balanced trade-off between spatial and spectral information in the fused result is desirable. This study demonstrates an effective mechanism for pan-sharpening multi-spectral images, which is referred to as convolutional sparse representation (CSR). Furthermore, the CSR approach produces such promising results while keeping the associated computational complexity to a minimum. The fused image is assessed both with and without the usage of a reference image. The first requires image downscaling, whereas the latter is done at native scale. The experimental part shows how the CSR-based PS approach may provide a desired HRMS image with limited computational resources.

Conflict of interest:

The authors note that they have no known competing financial or personal interests that would have influenced the findings of this study.

References:

- [1]. L. Alparone, B. Aiazzi, S. Baronti, and A. Garzelli, "Remote sensing image fusion" CRC Press, 2015. <https://doi.org/10.1201/b18189>
- [2]. X. Huang, L. Zhang, and P. Li, "Classification and extraction of spatial features in urban areas using high-resolution multispectral imagery," *IEEE Geoscience and Remote Sensing Letters*: 4/2 (2007) 260- 264. <https://doi.org/10.1109/LGRS.2006.890540>
- [3]. C. Thomas, T. Ranchin, L. Wald, and J. Chanussot, "Synthesis of multispectral images to high spatial resolution: A critical review of fusion methods based on remote sensing physics," *IEEE Transactions on Geoscience and Remote Sensing*: 46/5 (2008) 1301-1312. <https://doi.org/10.1109/TGRS.2007.912448>
- [4]. G. Vivone, L. Alparone, J. Chanussot, M. Dalla Mura, A. Garzelli, G. A. Licciardi, R. Restaino, and L. Wald, "A critical comparison among pan-sharpening algorithms," *IEEE Transactions on Geoscience and Remote Sensing*: 53/5 (2014) 2565-2586. <https://doi.org/10.1109/TGRS.2014.2361734>
- [5]. T.-M. Tu, P. S. Huang, C.-L. Hung, and C.-P. Chang, "A fast intensity hue- saturation fusion technique with spectral adjustment for IKONOS imagery," *IEEE Geoscience and Remote sensing letters*: 1/4 (2004) 309-312. <https://doi.org/10.1109/LGRS.2004.834804>
- [6]. C. A. Laben and B. V. Brower, "Process for enhancing the spatial resolution of multi-spectral imagery using pan-sharpening," US Patent 6, 011,875; Jan. 04, 2000.
- [7]. X. Otazu, M. GonzalezAud_cana, O. Fors, and J. Nunez, "Introduction of sensor spectral response into image fusion methods. application to wavelet-based methods," *IEEE Transactions on Geoscience and Remote Sensing*: 43/10 (2005) 2376-2385. <https://doi.org/10.1109/TGRS.2005.856106>
- [8]. S. S. Chen, D. L. Donoho, and M. A. Saunders, "Atomic decomposition by basis pursuit," *SIAM review*: 43/1 (2001) 129-159. <https://doi.org/10.1137/S003614450037906X>
- [9]. M. Elad, M. A. Figueiredo, and Y. Ma, "On the role of sparse and redundant representations in image processing," *Proceedings of the IEEE*: 98/6 (2010) 972-982. <https://doi.org/10.1109/JPROC.2009.2037655>
- [10]. M. Elad, "Sparse and redundant representations: from theory to applications in signal and image processing" Springer Science & Business Media, 2010.

- [11]. D. L. Donoho, "Compressed sensing," *IEEE Transactions on information theory*: 52(4) (2006) 1289-1306. <https://doi.org/10.1109/TIT.2006.871582>
- [12]. A. M. Bruckstein, D. L. Donoho, and M. Elad, "From sparse solutions of systems of equations to sparse modelling of signals and images," *SIAM review*: 51/1 (2009)81. <https://doi.org/10.1137/060657704>
- [13]. J. A. Tropp, "Greed is good: Algorithmic results for sparse approximation" *IEEE Transactions on Information theory*: 50/10 (2004) 2231-2242. <https://doi.org/10.1109/TIT.2004.834793>
- [14]. S. Li and B. Yang, "A new pan-sharpening method using a compressed sensing technique," *IEEE Transactions on Geoscience and Remote Sensing*: 49/2 (2011) 738-746. <https://doi.org/10.1109/TGRS.2010.2067219>
- [15]. Cheng, M. Wang, C. & Li, J. "Sparse representation based pan-sharpening using trained dictionary" *IEEE Geoscience and Remote Sensing Letters*: 11 (2014) 293-297. <https://doi.org/10.1109/LGRS.2013.2256875>
- [16]. Gogineni, R. & Chaturvedi, A. "Sparsity inspired pan-sharpening technique using multi-scale learned dictionary" *ISPRS Journal of Photogrammetry and Remote Sensing*: 146 (2018) 360-372. <https://doi.org/10.1016/j.isprsjprs.2018.10.009>
- [17]. Zhu, X. X. & Bamler, R. A "Sparse image fusion algorithm with application to pan-sharpening" *IEEE transactions on geoscience and remote sensing*: 51 (2013) 2827-2836. <https://doi.org/10.1109/TGRS.2012.2213604>
- [18]. Vicinanza, M. R.; Restaino, R.; Vivone, G.; Dalla Mura, M. & Chanussot, J. "A pan-sharpening method based on the sparse representation of injected details" *IEEE Geo-science and Remote Sensing Letters*: 12 (2015) 180-184. <https://doi.org/10.1109/LGRS.2014.2331291>
- [19]. Ayas, S.; Gormus, E. T. & Ekinci, M. "An Efficient Pan Sharpening via Texture Based Dictionary Learning and Sparse Representation" *IEEE Journal of Selected Topics in Applied Earth Observations and Remote Sensing*: 11/7 (2018) 2448-60. <https://doi.org/10.1109/JSTARS.2018.2835573>
- [20]. Shilesh Panchal, Rajesh Thakker, "Improved Image Pansharpening Technique using Nonsampled Contourlet Transform with Sparse Representation," *Journal of the Indian Society of Remote Sensing*, July 2016, pp 1-10, Online ISSN: 0974-3006, Springer India.
- [21]. Shilesh Panchal, Rajesh Thakker, "Contourlet Transform with Sparse Representation-Based Integrated approach for image pansharpening, *Journal IETE Journal of Research*, Pages 1-11, May 2017. <https://doi.org/10.1080/03772063.2017.1326294>
- [22]. Zeiler MD, Krishnan D, Taylor GW, Fergus R. "Deconvolutional networks" In 2010 IEEE Computer Society Conference on computer vision and pattern recognition 2010 Jun 13 (pp. 2528-2535). <https://doi.org/10.1109/CVPR.2010.5539957>
- [23]. Gogineni R, Chaturvedi A. A robust pansharpening algorithm based on convolutional sparse coding for spatial enhancement. *IEEE Journal of Selected Topics in Applied Earth Observations and Remote Sensing*. 2019 Nov 1; 12(10):4024-37. <https://doi.org/10.1109/JSTARS.2019.2945815>
- [24]. B. Wohlberg, "Efficient algorithms for convolutional sparse representations" *IEEE Transactions on Image Processing*: 25/1 (2015) 301-315. <https://doi.org/10.1109/TIP.2015.2495260>
- [25]. S. Boyd, N. Parikh, E. Chu, B. Peleato, J. Eckstein. "Distributed optimization and statistical learning via the alternating direction method of multipliers" *Foundations and Trends R in Machine learning*, 3/1 (2011) 1122. <https://doi.org/10.1561/22000000016>
- [26]. L. Wald, T. Ranchin, and M. Mangolini, "Fusion of satellite images of different spatial Resolutions: Assessing the quality of resulting images," *Photogrammetric engineering and remote sensing*: 63/6 (1997) 691-699.
- [27]. L. Alparone, B. Aiazzi, S. Baronti, A. Garzelli, F. Nencini, and M. Selva, "Multispectral and panchromatic data fusion assessment without reference" *Photogrammetric Engineering & Remote Sensing*: 74/2 (2008) 193-200. <https://doi.org/10.14358/PERS.74.2.193>
-